



This is a repository copy of *Fringing in tubular permanent-magnet machines: Part II. Cogging force and its minimization* .

White Rose Research Online URL for this paper:
<http://eprints.whiterose.ac.uk/828/>

Article:

Wang, J.B., Howe, D. and Jewell, G.W. (2003) Fringing in tubular permanent-magnet machines: Part II. Cogging force and its minimization. *IEEE Transactions on Magnetics*, 39 (6). pp. 3517-3522. ISSN 0018-9464

<https://doi.org/10.1109/TMAG.2003.819449>

Reuse

Unless indicated otherwise, fulltext items are protected by copyright with all rights reserved. The copyright exception in section 29 of the Copyright, Designs and Patents Act 1988 allows the making of a single copy solely for the purpose of non-commercial research or private study within the limits of fair dealing. The publisher or other rights-holder may allow further reproduction and re-use of this version - refer to the White Rose Research Online record for this item. Where records identify the publisher as the copyright holder, users can verify any specific terms of use on the publisher's website.

Takedown

If you consider content in White Rose Research Online to be in breach of UK law, please notify us by emailing eprints@whiterose.ac.uk including the URL of the record and the reason for the withdrawal request.



eprints@whiterose.ac.uk
<https://eprints.whiterose.ac.uk/>

Fringing in Tubular Permanent-Magnet Machines: Part II. Cogging Force and Its Minimization

Jiabin Wang, *Member, IEEE*, David Howe, and Geraint W. Jewell

Abstract—In Part I of the paper, analytical field solutions, which account for the fringing flux associated with the finite length of the ferromagnetic armature core in tubular permanent-magnet machines, are established. In Part II, the technique is applied to both slotless and slotted machines, and the results are verified by finite-element calculations. The analytical field solutions enable the resultant cogging force associated with the finite length of the armature to be determined as a function of the armature displacement, for both radially and Halbach magnetized stators. Thus, they not only provide an effective means for evaluating the influence of leading design parameters on the cogging force waveform, but also facilitate its minimization.

Index Terms—Cogging force minimization, linear machines, permanent-magnet machines.

I. INTRODUCTION

THE EFFECT OF fringing, associated with the finite length of the ferromagnetic armature core, on the flux-linkage, electromotive force (EMF), and thrust force of tubular permanent-magnet machines has been analyzed in Part I of the paper. However, the interaction of the permanent magnets with the finite-length armature core produces another undesirable effect—cogging force, which causes the armature to align in a position that corresponds to minimum magnetic energy when unexcited. This component of cogging force results primarily from the normal forces F_l and F_r , which are developed on each end face of the armature core, as illustrated in Fig. 1. The two components are unidirectional and act in opposite directions. For tubular permanent-magnet machines that have a slotted armature, there exists a second component of cogging force that is caused by the interaction of the permanent-magnet field with the permeance function of the slotted core. If not reduced to an acceptable level, the cogging force will have a destabilizing effect on the servo control system and compromise position and speed control accuracy.

With regards to the cogging force component due to slotting, most cogging force reduction techniques [1]–[5] that are employed for rotary permanent-magnet machines are effective. However, they are not effective for reducing the cogging force component associated with the finite core length since this has a different wavelength from the component due to slotting, namely, one pole pitch cf. one tooth-pitch. To overcome this

problem, a different technique, which utilizes the fact that the cogging force components at each end of the armature are unidirectional and act in opposite directions, has been proposed [6]. By optimizing the armature core length, the cogging force components associated with both ends can cancel each other. In order to apply this technique, however, a knowledge of the variation of the cogging force component at one end of the armature as a function of armature position over a half-pole pitch period is required. Although this relationship can be obtained by numerical techniques, such as finite-element analysis, it remains time consuming, particularly in a design optimization process when different combinations of design parameters are being considered.

Utilizing the analytical field solutions that have been established in Part I, the single-ended and resultant cogging forces can be determined as functions of the armature displacement, for both radial and Halbach magnetized tubular machine topologies. Thus, they not only provide an effective means for evaluating the influence of leading design parameters on the cogging force waveform, but also facilitate its minimization.

II. COGGING FORCE PREDICTION

The finite length of the armature core results in a cogging force that is dependent only on the relative position between the armature and the stator magnets. The cogging force acting at one end of the armature is unidirectional, and the net cogging force is the algebraic sum of the forces acting at both ends, as illustrated schematically in Fig. 1.

In Part I, the magnetic field distribution in region I of the analytical model of Fig. 1 was established for both radial and Halbach magnetized stators. For example, with radially magnetized magnets, the axial component of flux density in region I is given by

$$B_{Iz}(r, z) = - \sum_{j=1,2,\dots}^{\infty} [a_{Ij} B K_0(q_j r)] \cos q_j(z - \tau_a) \quad (1)$$

where $B K_0$ is a modified Bessel function of the second kind of order 0, $q_j = \pi j / \tau_l$, and the definition of the coefficient a_{Ij} is given in Appendix A of Part I. The single-ended cogging force can be derived by application of the virtual work principle. For example, the cogging force at the left end of the armature F_l is given by

$$F_l = \int \int_S \frac{1}{2} B \cdot H ds \quad (2)$$

Manuscript received March 26, 2002; revised May 9, 2003.

The authors are with the Department of Electronic and Electrical Engineering, University of Sheffield, Sheffield, South Yorkshire S1 3JD, U.K. (e-mail: j.b.wang@sheffield.ac.uk).

Digital Object Identifier 10.1109/TMAG.2003.819449

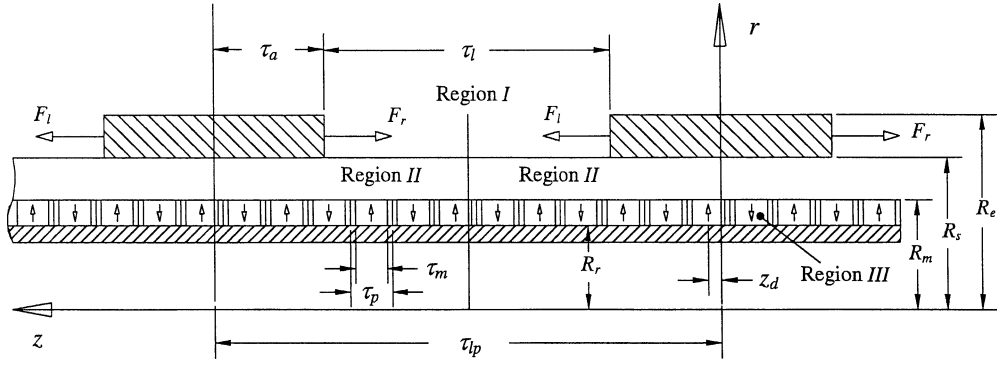


Fig. 1. Analytical model for cogging force calculation.

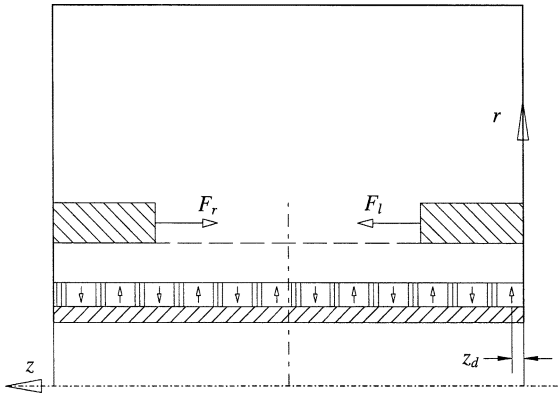


Fig. 2. Model for finite-element analysis.

where S denotes the left end surface of the armature core. Since at this surface, $z = \tau_a$, $B_{Ir} = 0$, (2) can be further simplified to

$$F_l = +\frac{\pi}{\mu_0} \int_{R_s}^{R_e} r B_{Iz}^2(r, \tau_a) dr \quad (3)$$

where R_e is the outer radius of the armature core. The positive sign in (3) indicates that the force acts in the direction of the z axis. Similarly, the cogging force at the right end of the armature is given by

$$F_r = -\frac{\pi}{\mu_0} \int_{R_s}^{R_e} r B_{Iz}^2(r, \tau_a + \tau_l) dr. \quad (4)$$

The resultant cogging force is, therefore, obtained as

$$F_{TC} = F_l + F_r = \frac{\pi}{\mu_0} \int_{R_s}^{R_e} r [B_{Iz}^2(r, \tau_a) - B_{Iz}^2(r, \tau_a + \tau_l)] dr. \quad (5)$$

Equation (5) may be rewritten as

$$F_{TC} = \frac{\pi}{\mu_0} \int_{R_s}^{R_e} r [B_{Iz}(r, \tau_a) - B_{Iz}(r, \tau_a + \tau_l)] \times [B_{Iz}(r, \tau_a + \tau_l) + B_{Iz}(r, \tau_a)] dr. \quad (6)$$

For a machine with radially magnetized magnets, this can be further simplified to

$$F_{TC} = \frac{4\pi}{\mu_0} \int_{R_s}^{R_e} r \left\{ \sum_{j=1,3,\dots} a_{Ij} B K_0(q_j r) \right\} \times \left\{ \sum_{j=2,4,\dots} a_{Ij} B K_0(q_j r) \right\} dr. \quad (7)$$

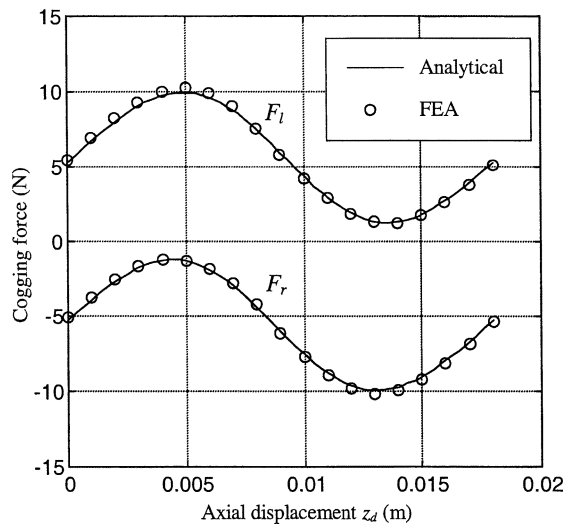
By replacing a_{Ij} with a_{pIj} , (7) is also applicable to a machine equipped with Halbach magnetized magnets.

For a given displacement z_d , between the armature and the stator magnets, as shown in Fig. 1, the equations in Appendixes A and B of Part I are used to determine the harmonic coefficients and, subsequently, the single-ended and resultant cogging forces, using (3), (4), and (7). This process is repeated for various values of z_d so as to obtain F_l , F_r , and F_{TC} as functions of z_d for a given set of machine parameters.

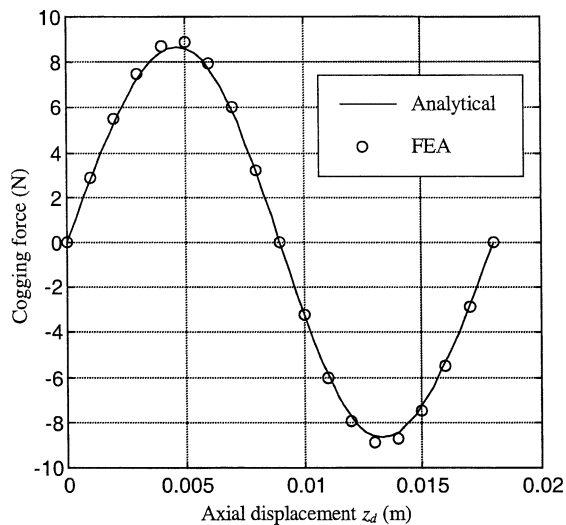
III. VALIDATION BY FINITE-ELEMENT ANALYSIS

The foregoing analytical scheme for calculating the cogging force is applied to both radial and Halbach magnetized slotless machines, whose leading design parameters are given in Table I of Part I. The magnets are sintered NdFeB with $B_{rem} = 1.15$ T and $\mu_r = 1.07$. The outer radius of the armature core R_e is 0.035 m. The results obtained from the analytical prediction are validated by finite-element analysis using the model shown in Fig. 2. Since cogging force may be sensitive to the relative permeability of the stator and armature cores, the magnetic field is solved using the nonlinear model in which the material properties of the cores are represented by their respective B-H curves, and a periodic condition is imposed at the axial boundaries $z = 0$ and $z = \tau_{lp}$. The resulting cogging force is calculated using both Maxwell stress integration and the change in coenergy with respect to the displacement of the armature.

Fig. 3(a) compares the cogging force components in the radially magnetized machine as a function of the axial position z_d , while Fig. 3(b) compares the resultant cogging force that acts on the armature core. Similar comparisons are presented in Fig. 4(a) and (b) for the Halbach magnetized machine. As will be seen, the analytical predictions agree well with the finite-element results, the maximum error being less than 3%,



(a)

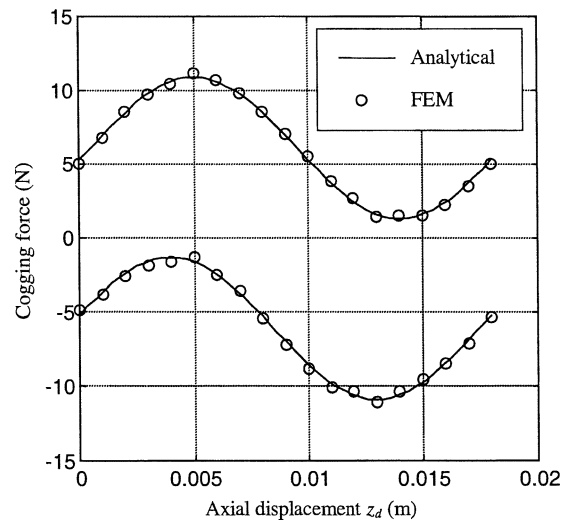


(b)

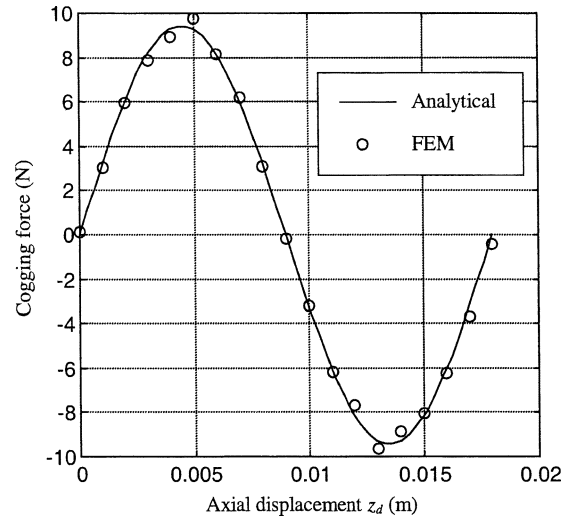
Fig. 3. Comparison of cogging force components and resultant cogging force as a function of axial displacement z_d in radially magnetized machine. (a) Cogging force components. (b) Resultant cogging force.

which may be attributable to discretization effects, and the non-linear magnetization curve and finite permeability of the iron in the finite-element analysis. It will be noted that the cogging force is relatively sensitive to the accuracy of the magnetic field solution. Thus, attention must be paid to the accuracy of the flux density components in both the analytical and FE calculations. In this regard, the FE mesh must be relatively fine in the air-gap region close to the armature core, while for the analytical prediction, the number of harmonic terms must be sufficiently high. Fig. 5 shows the variation of the root-mean-square (rms) error, over a half pole pitch between the FE and analytically calculated cogging force as a function of the number of harmonics for the radially magnetized machine. As can be seen, in this particular case an increase in the number of harmonics beyond ~ 25 does not result in a reduction in the rms error.

Since the armature core length used in the calculation is 0.072 m and equal to four (i.e., an integer number) pole pitches, the single-ended cogging force components F_l and F_r are the



(a)



(b)

Fig. 4. Comparison of cogging force components and resultant cogging force as a function of axial displacement z_d in Halbach magnetized machine. (a) Cogging force components. (b) Resultant cogging force.

mirror image of each other [6]. This relationship is clearly evident in Figs. 3(a) and 4(a), although slight discrepancies exist in the finite-element results. It can also be observed that the waveforms of the single-ended cogging force components are almost symmetrical with respect to the axial position at which the peak value occurs. This symmetry is useful for the minimization of the resultant cogging force.

IV. COGGING FORCE MINIMIZATION

Since the cogging force components that act at each end of the armature are unidirectional and in opposition, it is possible to select an optimum armature core length such that the resultant cogging force waveform as a function of the axial displacement z_d has a minimum peak value. The optimal core length may be obtained by evaluating the cogging force waveform using the analytical technique described in Section II by varying the core length. However, a more efficient approach is to determine the optimal core length described as follows [6].

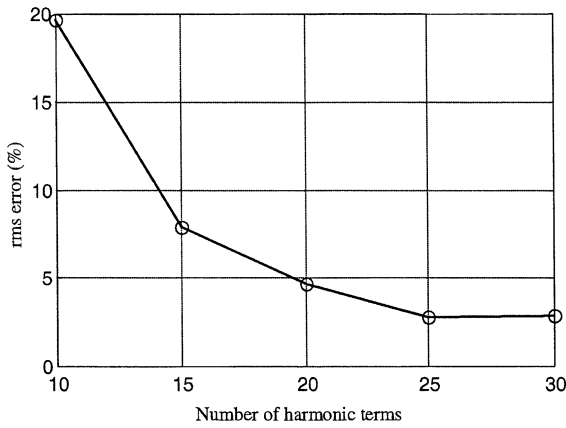
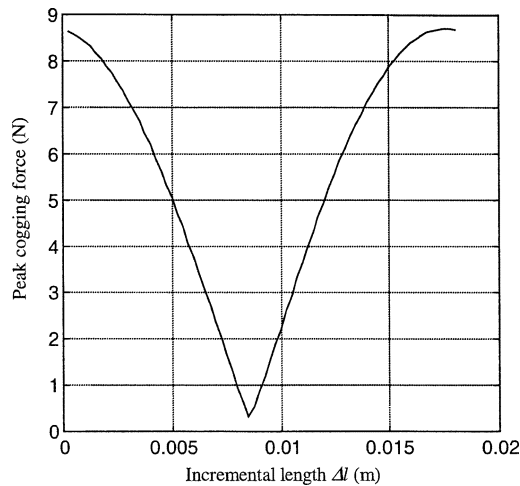
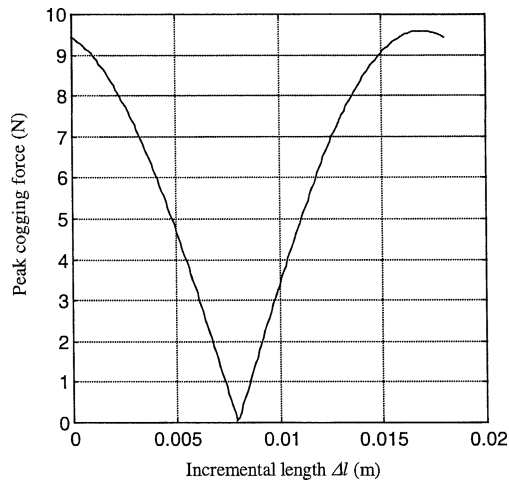


Fig. 5. Variation of rms error over a half pole pitch between FE and analytical calculations as a function of number of harmonics for radially magnetized machine.



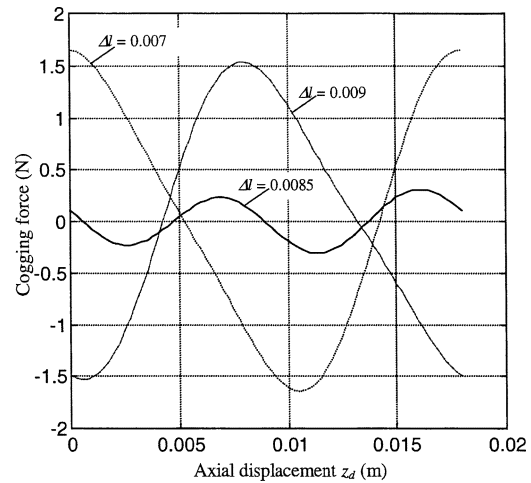
(a)



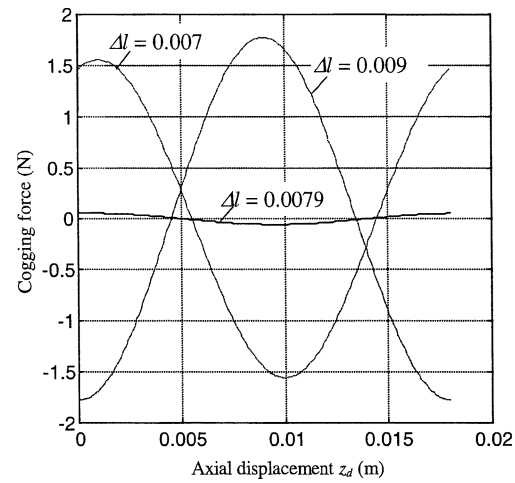
(b)

Fig. 6. Variation of peak cogging force as a function of incremental length Δl . (a) Radially magnetized magnets. (b) Halbach magnetized magnets.

If $F_r(z_d)$ and $F_l(z_d)$ are the calculated cogging force components for an armature core length l_e , which is equal to an integer multiple of pole pitches, the two functions will vary periodically with respect to z_d , the period being equal to a pole pitch. Thus, the cogging force components $F_{l+\Delta l}(z_d)$ and $F_{r+\Delta l}(z_d)$, asso-



(a)



(b)

Fig. 7. Cogging forces as a function of axial position for three different values of incremental length. (a) Radially magnetized magnets. (b) Halbach magnetized magnets.

ciated with a core length $(l_e + \Delta l)$, where Δl denotes an arbitrary increment, can be obtained as

$$\begin{aligned} F_{l+\Delta l}(z_d) &= F_l(z_d) \\ F_{r+\Delta l}(z_d) &= F_r(z_d + \Delta l). \end{aligned} \quad (8)$$

The resultant cogging force $F_{CT+\Delta l}(z_d)$ is, therefore, given by

$$F_{CT+\Delta l}(z_d) = F_l(z_d) + F_r(z_d + \Delta l). \quad (9)$$

When the waveforms of $F_r(z_d)$ and $F_l(z_d)$ are determined using (3) and (4) over a displacement of a half pole pitch, the complete waveforms for a displacement over one pole pitch can be obtained by taking the mirror image of each component. Hence, $F_{r+\Delta l}(z_d)$ can be obtained for any incremental length Δl . By varying the value of Δl over a pole pitch, an optimal incremental length Δl_o that results in a minimum peak value for $F_{CT+\Delta l}(z_d)$ can easily be found.

Fig. 6(a) shows the variation of the peak cogging force as a function of the incremental length Δl for the radially magnetized machine with the same parameters as stated earlier. A similar cogging force variation is presented in Fig. 6(b) for the Halbach magnetized machine. It is evident that there

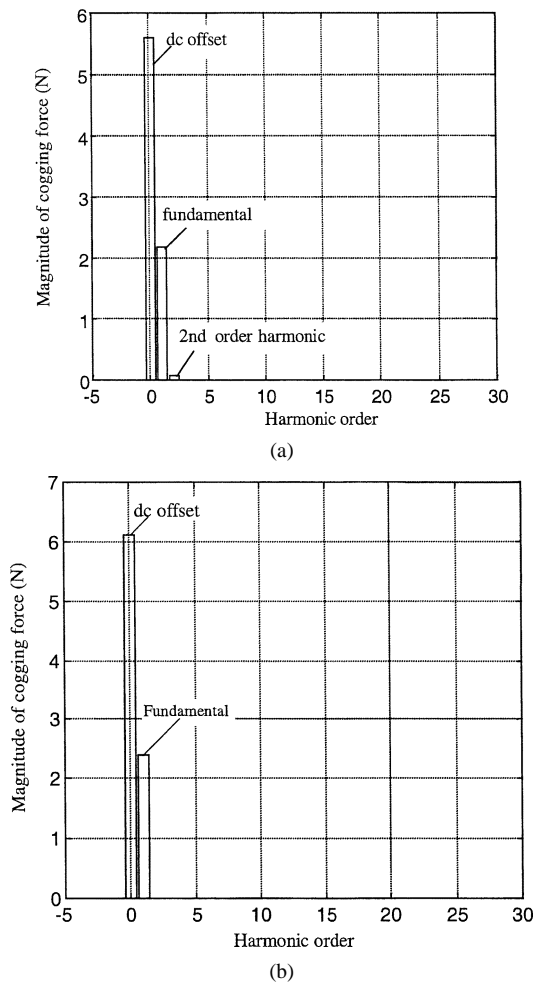


Fig. 8. Harmonic distribution of single-end cogging force waveforms with slotless armature. (a) Radially magnetized magnets. (b) Halbach magnetized magnets.

is a clearly defined optimal incremental length Δl for both machines, which results in a minimum peak value for the resultant cogging force. The optimal values are 0.0085 and 0.0079 m for the radial and Halbach magnetized machines, respectively, and the corresponding peak cogging forces are 0.34 and 0.053 N. It will be noted that although the Halbach magnetized machine with $\Delta l = 0$ has a higher peak cogging force than the radially magnetized machine, the former has a much lower minimum peak cogging force than the latter.

Fig. 7(a) and (b) shows the cogging force waveforms that result from three different values of incremental length for the armatures of the two machines. As will be seen, the cogging force waveforms in Fig. 7(a) for the radially magnetized machine are not symmetrical when $\Delta l = 0.007$ and 0.009 m. Consequently, the cogging force can never be eliminated completely. For the Halbach magnetized machine, however, the cogging force waveforms that result with $\Delta l = 0.007$ and 0.009 m are both symmetrical, with a period of one pole pitch. This makes it possible, at least in theory, to reduce the cogging force to zero. This is due to the intrinsic sinusoidal magnetization distribution in the Halbach magnetized magnets. As a result, the single-ended cogging force is also sinusoidally distributed with a dc offset, as can be seen from the harmonic distribution in

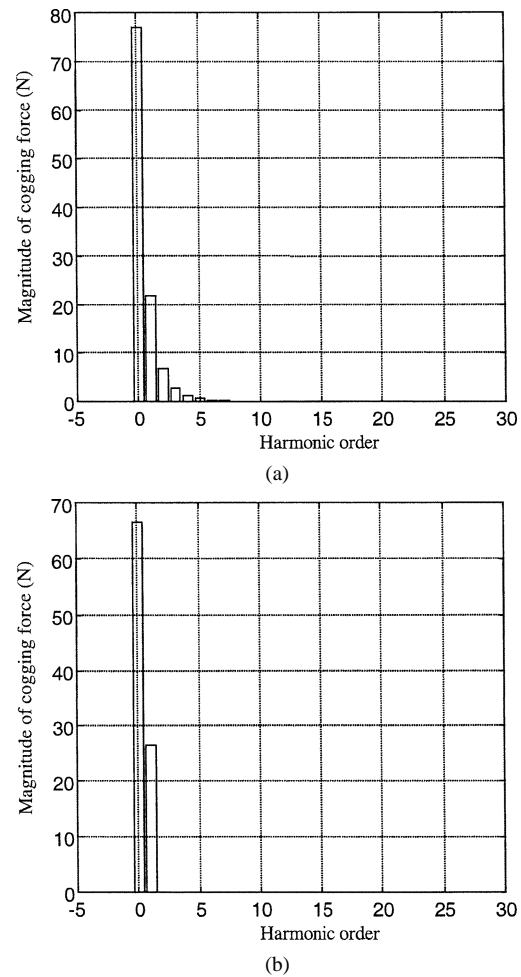


Fig. 9. Harmonic distributions of single-end cogging force waveforms with slotted armature. (a) Radially magnetized. (b) Halbach magnetized.

Fig. 8 for the cogging force waveform that acts at the left-hand side of the armature $F_l(z_d)$. In contrast, the single-end cogging force waveform for the radially magnetized machine contains a noticeable second-order harmonic that continues to be present when the incremental length Δl is optimized to eliminate the fundamental component of cogging force.

For the radially magnetized machine, the high-order cogging force components become more significant as the radial thickness of the air gap/winding region is reduced. Fig. 9(a) shows the harmonic distribution of the single-end cogging force for a machine having a small air gap, which is equivalent to that of the slotted machine whose leading design parameters are given in Table I of Part I. Due to the existence of such relatively high-order harmonics, it is difficult to reduce the end-effect component of cogging force to an acceptable level simply by varying the incremental length Δl . For the Halbach magnetized machine, however, since the single-end cogging force waveform contains only a dc offset and a fundamental component, even with a small air gap, as shown in Fig. 9(b), it is possible to eliminate not only the end component of cogging force by optimizing the armature core length, but also the cogging force due to slotting by choosing an appropriate slot opening. Hence, a slotted Halbach magnetized machine can be designed to have an extremely low cogging force while having a high force capability.

V. CONCLUSION

An analytical expression for predicting the component of cogging force that results from the finite length of an iron-cored armature in a tubular permanent-magnet machine has been established, and a technique for minimizing the cogging force has been described. These have been applied to machines equipped with radial magnetized and Halbach magnetized stators. It has been shown that for a machine with Halbach magnetized magnets, it is possible to completely eliminate the cogging force by choosing an appropriate armature length. In contrast, complete elimination of the cogging force using this technique is not possible for the machines having radially magnetized magnets, particularly when the effective gap between the magnets and the armature core is relatively small, as with a slotted armature.

REFERENCES

- [1] T. Li and G. Slemon, "Reduction of cogging torque in permanent magnet motors," *IEEE Trans. Magn.*, vol. 24, pp. 2901–2903, Nov. 1988.
 - [2] B. Ackerman, J. H. Janssen, R. Sottek, and R. I. Van Steen, "A new method for reducing cogging torque in a class of brushless DC motors," *Proc. Inst. Elect. Eng.—Electr. Power Appl.*, vol. 139, no. 4, pp. 138–145, 1992.
 - [3] S. Hwang and D. K. Lieu, "Design techniques for reduction of reluctance torque in brushless permanent magnet motors," *IEEE Trans. Magn.*, vol. 30, pp. 4287–4289, Nov. 1994.
 - [4] S. K. Chang, S. Y. Hee, W. N. Ki, and S. C. Hong, "Magnetic pole shape optimization of permanent magnet motor for reduction of cogging torque," *IEEE Trans. Magn.*, vol. 33, pp. 822–827, Mar. 1997.
 - [5] Y. T. Wanata, M. Torri, and D. Ebihara, "Study on the reduction of detent force of permanent magnet linear synchronous motor," in *Proc. LDIA'95*, Nagasaki, Japan, 1995, pp. 207–210.
 - [6] Z. Q. Zhu, Z. P. Xia, D. Howe, and P. H. Mellor, "Reduction of cogging force in slotless linear permanent magnet motors," *Proc. Inst. Elect. Eng.—Electr. Power Appl.*, vol. 144, no. 4, pp. 277–282, 1997.
 - [7] J. Wang, D. Howe, and G. W. Jewell, "Fringing in tubular permanent-magnet machines: Part I. Magnetic field distribution, flux linkage, and thrust force," *IEEE Trans. Magn.*, vol. 39, pp. 3507–3516, Nov. 2003.
- Jiabin Wang** (M'96) was born in Jiangsu Province, China, in 1958. He received the B.Eng. and M.Eng degrees from Jiangsu University of Science and Technology, Zhengjiang, China, and the Ph.D. degree from the University of East London, London, U.K., in 1982, 1986, and 1996, respectively, all in electrical and electronic engineering.
- From 1986 to 1991, he was with the Department of Electrical Engineering, Jiangsu University of Science and Technology, where he was appointed a Lecturer in 1987 and an Associated Professor in 1990. He was a Post-Doctoral Research Associate at the University of Sheffield, Sheffield, U.K., from 1996 to 1997 and a Senior Lecturer at the University of East London from 1998 to 2001. He is currently a Senior Lecturer at the University of Sheffield. His research interests range from motion control to electromagnetic devices and their associated drives.
- David Howe** received the B.Tech and M.Sc. degrees from the University of Bradford, Bradford, U.K., and the Ph.D. degree from the University of Southampton, Southampton, U.K., in 1966, 1967, and 1974, respectively, all in electrical power engineering.
- He has held academic posts at Brunel and Southampton Universities, and spent a period in industry with NEI Parsons Ltd. working on electromagnetic problems related to turbo-generators. He is currently a Professor of Electrical Engineering at the University of Sheffield, Sheffield, U.K., where he heads the Electrical Machines and Drives Research Group. His research activities span all facets of controlled electrical drive systems, with particular emphasis on permanent-magnet excited machines.
- Prof. Howe is a Chartered Engineer in the U.K. and a Fellow of the Institution of Electrical Engineers, U.K.
- Geraint W. Jewell** was born in Neath, Wales, U.K., in 1966. He received the B.Eng. and Ph.D. degrees from the Department of Electronic and Electrical Engineering, University of Sheffield, Sheffield, U.K., in 1988 and 1992, respectively.
- From 1994 to 2000, he was a Lecturer in the Electrical Machines and Drives Research Group, University of Sheffield, where he currently holds an Engineering and Physical Sciences Research Council Advanced Research Fellowship. His research interests cover many aspects of both permanent-magnet and reluctance-based electrical machines and actuators.